Recent Advances in Optical Tweezers

Jeffrey R. Moffitt,[1] Yann R. Chemla,[3] Steven B. Smith,[1] and Carlos Bustamante[1,2]

[1]Department of Physics, [2]Departments of Chemistry, and Molecular and Cell Biology and Howard Hughes Medical Institute, University of California, Berkeley, California 94720; email: carlos@alice.berkeley.edu

[3]Department of Physics, University of Illinois, Urbana-Champaign, Urbana, Illinois 61801

Annu. Rev. Biochem. 2008. 77:205–28

First published online as a Review in Advance on February 28, 2008

The *Annual Review of Biochemistry* is online at biochem.annualreviews.org

This article's doi: 10.1146/annurev.biochem.77.043007.090225

0066-4154/08/0707-0205$20.00

Key Words

force, hybrid-instruments, molecular motors, single molecule, torque

Abstract

It has been over 20 years since the pioneering work of Arthur Ashkin, and in the intervening years, the field of optical tweezers has grown tremendously. Optical tweezers are now being used in the investigation of an increasing number of biochemical and biophysical processes, from the basic mechanical properties of biological polymers to the multitude of molecular machines that drive the internal dynamics of the cell. Innovation, however, continues in all areas of instrumentation and technique, with much of this work focusing on the refinement of established methods and on the integration of this tool with other forms of single-molecule manipulation or detection. Although technical in nature, these developments have important implications for the expanded use of optical tweezers in biochemical research and thus should be of general interest. In this review, we address these recent advances and speculate on possible future developments.

Contents

PROLOGUE

Light carries both linear and angular momentum and can thus exert forces and torques on matter. Optical tweezers exploit this fundamental property to trap objects in a potential well formed by light (1, 2). This technique allows the manipulation of microscopic objects in applications ranging from particle sorting (3) to microfabrication (4, 5). Moreover, optical tweezers can be used as quantitative tools to exert calibrated forces on systems of interest as well as accurately and sensitively measure the forces and displacements generated by these systems. Such analytical optical tweezers have been used in a variety of applications ranging from microrheology (6) to the study of colloidal hydrodynamics (7–10) and nonequilibrium thermodynamics (11–16). More importantly, analytical optical tweezers have developed into a powerful tool in molecular biology, biochemistry, and biophysics, where they are used to manipulate and interrogate individual molecules. From these studies, scientists are gaining essential new insights into the mechanical properties of biological macromolecules and the dynamics and mechanisms of molecular motors—the proteins and complexes of proteins that use chemical energy to perform mechanical tasks in the cell.

In the past decade and a half, it has become increasingly evident that force is involved in many facets of cellular life, ranging from the obvious—the transport of cellular cargo by motors, such as myosin, kinesin, and dynein—to the more subtle and speculative, such as the strain induced on an enzyme and its substrate during catalysis (17). With the ability to

apply forces on individual molecules and measure the forces generated in their chemical reactions, analytical optical tweezers are ideally suited to investigate such mechanochemical transformations. However, despite their unique contributions to the study of single-molecule processes, these techniques have had limitations. First, they have lacked the sensitivity to study many of these molecular processes at their fundamental spatiotemporal scales—the angstrom to nanometer distance scales and millisecond to second timescales. Second, studies using these methods have largely been limited to simple biological systems, consisting only of a few components observed in isolation, far from their native cellular context. It has become clear that to capture the full complexity of the cell and its components, a new experimental toolset will be needed, capable of manipulating more complicated biological systems and measuring their conformation changes with greater sensitivity.

In recent years, parallel advances in optical trapping methodologies have aimed at addressing these limitations, on one hand improving the resolution and accuracy of current instrumentation, and on the other developing new hybrid instruments, which combine various single-molecule techniques for the manipulation of complex systems and the simultaneous measurement of multiple observables. In this review, we discuss this next generation of instrumentation and its potential for deepening our understanding of fundamental biological processes. Because these developments are inherently technical, this review requires some knowledge of optical tweezers: the principles by which they function and the basic instrumentation required to build them. To assist readers new to this topic, we start with a brief introduction to optical trapping, and throughout we refer the interested reader to the excellent literature on this subject. Following this introduction, we discuss the recent technical and theoretical advances that have refined the resolution of analytical optical tweezers, culminating in the ability to detect, for the first time, motions of biological systems as small as a few angstroms on the one-second timescale, with accuracy approaching a few percent. In parallel to this development, there has been significant effort to generalize the traditional optical tweezers by incorporating them with other forms of single-molecule manipulation and detection. Thus, in the third section of this review, we discuss this current work and the biological problems that have motivated these developments. Finally, we conclude with some speculation on what the future holds for the development and application of optical tweezers in the study of complex biological systems.

INTRODUCTION TO OPTICAL TWEEZERS

The physical principles behind optical trapping are relatively simple and straightforward as are the instrumentation techniques necessary to build a standard optical tweezers. In this introductory section, we briefly review the basic principles of optical trapping to aid those new to the field and throughout refer to additional reading in the literature. Readers familiar with this topic may want to skip this section.

How Do You Trap?

Optical traps involve the balance of two types of optical forces: scattering forces, which push objects along the direction of propagation of the light, and gradient forces, which pull objects along the spatial gradient of light intensity (2). When gradient optical forces exceed those from scattering, an object is attracted to the point of highest intensity formed by focused light and can be stably trapped at this position in all three dimensions (2). In practical implementations of an optical trap, a near-infrared laser beam is tightly focused by a high-numerical aperture microscope objective to create the large spatial gradient in light intensity necessary to form a stable trap (18). In the vicinity of this focus, the optical trap

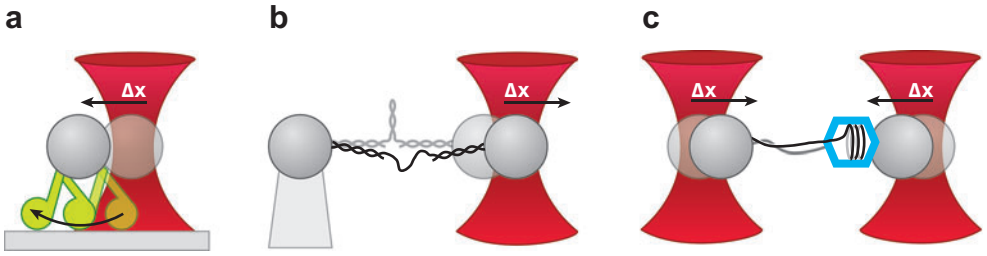

Figure 1

Different experimental geometries for optical tweezers. (*a*) For processive cytoskeletal motors, such as kinesin, the motor is typically attached directly to a polystyrene bead held in an optical trap, and the filament is attached to the surface of a sample chamber. Motions of the motor are revealed by motions of the trapped bead. (*b*) It is also possible to attach one end of the biological system to a second polystyrene bead suctioned onto the end of a micropipette. The motion of the biological system, such as the unfolding of a RNA hairpin, is again revealed in the motion of the trapped bead. (*c*) The second bead can also be held in a second optical trap. In this case, changes in the length of the tethered DNA by the action of a bacteriophage portal motor are revealed in the motions of both beads. The relative motion of each bead depends on the relative stiffness of the two optical traps.

behaves as a linear "Hookean" spring, generating forces on an object proportional to its displacement from the center of the trap.

How Do You Manipulate?

Back-focal-plane interferometry: detection method that uses the interference pattern formed between the trapping laser and the scattered light to measure bead movements

The magnitude of these optical forces is generally insufficient to stably trap biological macromolecules themselves, but more than adequate for manipulating microscopic dielectric objects,[1] such as micron-sized polystyrene beads, which can be biochemically linked to these molecules of interest. In the majority of single-molecule optical tweezers experiments, these beads serve as handles to a biological system, allowing its manipulation inside a sample chamber. Exerting calibrated forces on this molecule usually requires that the biological system is also attached at the other end. Typically this second attachment point is the surface of a sample chamber (**Figure 1*a***), a second bead held atop a micropipette by suction (**Figure 1*b***), or a bead held in a second optical trap (**Figure 1*c***) (19–21). In this fashion, the system can be stretched by moving the optical trap relative to the attachment point. The tether itself may be a molecular motor, such as kinesin or myosin (22–24) (**Figure 1*a***), a molecule undergoing conformational transitions under tension, such as an RNA hairpin or protein (25–28) (**Figure 1*b***), or the substrate to a motor, such as a DNA molecule packaged by a viral portal motor (**Figure 1*c***) (20, 29).

How Do You Detect?

In each case, the action of the system—kinesin stepping along a microtubule, the RNA hairpin unfolding, or the viral packaging motor translocating DNA (**Figure 1*a-c***)—is monitored from the motions of the bead in the optical trap (or traps). Thus, the beads not only serve as handles to a biological system but also as probes by which its movements are inferred. The sensitive detection of the bead position in its trap and, by extension, the calibrated measurement of displacement and force constitute a key feature of analytical optical tweezers. Several methods for measuring the position of a trapped particle exist and have been covered extensively in the literature (18, 30). However, one technique, back-focal plane interferometry (31–33), has become the standard in the field owing to its sensitivity, linearity, and speed in all three dimensions.

[1]Typically, optical traps can generate forces of several picoNewtons (pN), or 1×10^{-12} Newtons, per milliwatt (mW) of laser light.

With this technique, it is in principle possible to detect bead motions of less than 1 Å on the timescale of a millisecond or better, limited only by the background electronic noise of the detector (34).

How Do You Measure?

Optical tweezers data, in its raw form, typically consist of various voltages from photodetectors and other components of the instrument. Thus, before quantitative measurements can be made, these raw data must be converted to the actual physical parameters of the system—the picoNewton forces exerted on and the nanometer displacements of the trapped bead. This calibration typically involves measuring the response of the trapped bead to a known force; however, there are methods for measuring the optical force directly (35). The standard calibration techniques are well reviewed in References 18 and 30.

Unfortunately, even with calibrated displacements and forces, these values alone cannot determine the actual motion of the biological system. It is often necessary to also know the elastic behavior of the tethered molecule and measure both its extension—the end-to-end distance from one attachment point to the other—and the tension—inferred from the optical force exerted on the bead by the trap (36, 37). An alternative technique that proves useful when the compliance of the tether or its extension or attachment point are not known is *force feedback*—a mode of operation in which the position of the optical trap relative to the second attachment point is adjusted to maintain a constant optical force on the bead at all times (38). In this case, the bead displacement within the trap remains fixed, and it is the displacement of the trap relative to the second attachment point that directly measures the change in extension of the molecule owing to the action of the biological system. In essence, a trap operated under force feedback has zero stiffness because motions of the attachment point relative to the trap do not result in changes in the applied force. Recent work has shown that it is possible to achieve the same effect optically by exploiting nonlinear regions of the trapping potential (39).

The ability to detect movements of the biological system, as inferred from the motions of the bead handles or the motion of the optical trap, defines the spatial resolution of the instrument, and the timescale of detectable motions defines its temporal resolution. As is discussed below, these two concepts are inextricably linked. In the following section, we review recent technical advances that have pushed the resolution of optical tweezers to the angstrom spatial scale on the second timescale. For readers interested in further discussion of optical tweezers and use of the standard assay for biological studies, see References 18–21, 26, 40–46.

IMPROVEMENTS IN RESOLUTION

Recently, major advances have been made in the development of ultrastable and low-noise optical tweezers. These developments have come not only in the form of better instrumentation and technique but also in a better understanding of the fundamental and physical limitations to the sensitivity of optical tweezers. In this section, we review these exciting advances.

Why Do You Want Better Resolution?

Many fundamental processes in the cell are mechanical in nature and occur by discrete physical movements, for example, the steps of molecular motors along cytoskeletal filaments, the incorporation of one nucleotide to a nascent nucleic acid chain in transcription or replication, or the unfolding and degradation of a protein domain by the proteasome. Often, the size of these displacements is dictated by the inherent periodicity of the substrate on which these systems act—the 8-nm repeat of microtubules or the 3.4-Å distance between

adjacent base pairs in double-stranded DNA (dsDNA). More generally, however, these processes can be viewed as reactions along an energy landscape in which the reaction coordinate corresponds to a physical distance (17, 47, 48). The discrete motion in these processes stems from the fact that the states along these reaction pathways are highly localized minima in this energy landscape. As a result, the direct observation and measurement of these discrete displacements, and deviations from this discreteness, can reveal important details on the energy landscape underlying these processes.

Although the size of such displacements is certainly of fundamental interest, the ability to detect discrete steps can also reveal detailed information on the governing kinetics. When discrete steps are obscured by experimental noise, one can at most measure the average rates of these processes and in some cases the fluctuations in these rates (48–50). By contrast, the direct detection of discrete steps allows one to measure the individual time intervals between these events—the dwell times—and in turn compile their full probability distribution. The dwell time distribution contains far more information than that available in the average rate, providing a statistical measure of the kinetics (48, 50). In the case of molecular motors, for instance, such techniques can be used to estimate the number of kinetic transitions in their mechanochemical cycles (48, 49); for motors with multiple subunits, they can also reveal the detailed coordination between the different subunits (51). With direct observation of the size and kinetics of the steps of a molecular motor, it is possible to reconstruct the detailed mechanism of the motor.

Unfortunately, these discrete movements have only been detectable by traditional optical trap measurements in limited instances. For cytoskeletal motors such as kinesin or myosin, the detection of steps is facilitated by the relatively large step sizes taken by these motors and by the experimental geometry in which the motor is directly tethered to the bead in the optical trap (**Figure 1*a***). In this situation, it is not uncommon to resolve steps of a few nanometers with dwells as short as only a few tens of milliseconds, resolution that is more than sufficient for the detailed study of these motors (22–24). By contrast, resolving the motions of molecular motors that translocate along nucleic acid is considerably more difficult, as these motors most likely move in steps on the single-base pair scale—a distance of only 3.4 Å on dsDNA. Moreover, some nucleic acid motors, such as the bacterial DNA translocase FtsK (52, 53), can be quite fast, moving with speeds as high as 3–5 kb/s and requiring high temporal resolution. Regrettably, the experimental geometries that use nucleic acid as a tether to the trapped bead (**Figure 1*b*,*c***) also suffer from worse spatial and temporal resolution, as described below. Thus, the detailed study of nucleic acid motors has required significant improvement in resolution over traditional techniques. Beyond their application to molecular motors, techniques with very high spatial and temporal resolution will be necessary to study the many protein conformational changes at the core of essential allosteric processes and enzymatic functions. Although protein conformational changes as big as several nanometers are rare, changes in the subnanometer range are ubiquitous. Thus, the ability to detect motions on the angstrom scale on a wide range of timescales, milliseconds to seconds, will allow the direct observation and study of the physical motions that underlie conformational changes in a wide class of proteins.

What Limits Resolution?

The spatial resolution of optical tweezers is limited by drift and noise from a variety of sources, which can be categorized as either experimental, i.e., all noise stemming from the environment or from components of the instrument, or Brownian, noise stemming from the fundamental thermal forces that generate the fluctuations of the trapped objects themselves. Experimental noise is typically

caused by drift and fluctuations in the sample stage or micropipette (**Figure 1**), resulting in motions of the trapped bead, which are indistinguishable from the motions generated by the biological system. Alternatively, motions of the optical trap itself or fluctuations in the laser power can lead to similar false signals. All of these problems can be addressed through better instrumentation (18, 34).

Thermal forces, by contrast, cannot be avoided and provide a fundamental limit to the resolution of a given experiment. To understand the origin of this limit, consider the forces acting on the optically trapped bead. At every moment in time, the bead positions itself in the optical trap to balance three forces: the force from the optical trap, the tension on the biological system, and the spontaneous and random thermal force from the aqueous environment surrounding the trapped bead.[2] To monitor the response of the biological system, the tension on the tether must be known, but this is never measured directly, only inferred from the measured optical force. Thus, this Brownian force introduces an uncertainty in the applied tension on the biological system, which fundamentally limits the resolution of an optical tweezers experiment. Fortunately, the effect of the Brownian force can be calculated, and experimental parameters can be tuned to reduce its effect as we discuss below. In practice, experimental noise sources must first be addressed before the instrument can attain a resolution limited only by fundamental Brownian noise.

How Do You Remove Experimental Noise?

The recent advances in high-resolution optical tweezers suggest that experimental noise mainly results from environmental factors. Temperature drift, mechanical and acoustic vibrations in the room, as well as background electronic noise, all can couple into the instrument and affect resolution (34). Criteria for selecting a quiet environment have been discussed in References 18 and 34. In addition to improving the instrument environment, techniques for addressing any remaining experimental noise have proven necessary to enhance the resolution of optical tweezers. In general, two approaches have been used: monitoring and subtracting this noise from measurements (55, 56) or designing the instrument such that it is isolated from or insensitive to these sources of noise (34, 36, 57, 58).

Detection laser: an additional focused laser beam used for detecting motion of a bead but not for trapping

In experimental layouts in which the surface of a sample chamber is the second attachment point (**Figure 1*a***), Nugent-Glandorf & Perkins (55) have shown that it is possible to monitor and correct for the drift and fluctuations in the environment by introducing a second detection laser (30) to monitor the position of the chamber surface. A fiducial mark is either deposited (55) or microfabricated (56) onto the chamber surface, allowing the detection laser to sensitively measure the position of this mark. Drift and fluctuations can then be removed by either subtracting the motion of this fiducial mark from the data or through active feedback of the stage position. Carter et al. (56) have recently demonstrated that this approach can stabilize a stage to better than 1 Å in three dimensions with a feedback bandwidth of 100 Hz. Approaches such as this should also be able to stabilize systems that use micropipettes (**Figure 1*b***).

The second approach is to isolate the instrument completely from the sample chamber by the use of two optical traps, as in **Figure 1*c*** (34, 36, 57, 58). Because the system of study is levitated above the chamber surface, slow drift in that surface has no effect on the measurement. Furthermore, by forming these dual traps from the same laser beam, the instrument can be effectively decoupled

[2] Viscous and inertial forces are typically negligible on the long timescales associated with the dynamics of most biological systems. For example, the inertial and viscous timescales for a 1-μm polystyrene bead, in a trap of stiffness 0.1 pN/nm, are ∼100 ns and ∼100 μs, respectively (54).

SNR: signal-to-noise ratio

from any drift in beam position. Remarkably, fluctuations in the two beam positions can still occur owing to slight changes in the index of refraction of the air from small density fluctuations and turbulence (34, 36, 58), in a similar fashion to the twinkling of stars at night. This atmospheric noise can be controlled either by housing the crucial optics in an atmosphere with a smaller index of refraction for which fluctuations produce smaller deviations in the beam direction, such as helium (34, 58), or in a partial vacuum, or by reducing the differential length of the optical paths traveled by the two lasers (34, 36). In this latter case, any atmospheric fluctuations in the common optical path will result in the same deviations for both beams, thus producing no change in the distance between the traps and no artifactual signals.

How Do You Address Brownian Noise?

As mentioned above, the thermal force that engenders Brownian motion is the second source of resolution-limiting noise and provides a fundamental limit to the resolution of an experiment, even in the absence of experimental noise. Although thermal fluctuations can never be completely eliminated, their dependence on experimentally tunable parameters, such as bead size and tether stiffness, allows their effect on resolution to be minimized. To this end, it is useful to understand how the resolution of an optical tweezers measurement depends on the choice of experimental parameters. A commonly used factor for assessing resolution is the signal-to-noise ratio (SNR), a dimensionless ratio of the size of a displacement signal to the noise that may obscure it (**Figure 2*a***). Although its derivation falls outside the scope of this review and has been extensively treated in the literature (36, 37), the expression for the SNR for an instrument with one optical trap, in measurements carried out on sufficiently slow timescales,[3] is illuminating:

$$SNR \leq \frac{\kappa_{tether}\Delta\ell}{\sqrt{4k_BTB\gamma}}, \qquad 1.$$

where κ_{tether} is the stiffness of the biological tether, i.e., the slope of the force-extension curve of the tether at a given tension, $\Delta\ell$ is the size of the physical displacement of the biological system, T is the temperature of the aqueous bath, k_B is the Boltzmann constant, B is the bandwidth of the measurement—half the rate at which data are collected, and $\gamma = 6\pi\eta r$ is the drag coefficient of the trapped bead. η is the viscosity of the medium, and r is the radius of the trapped bead. In the perfect instrument with no experimental noise, the observed SNR will be equal to the right-hand side of this equation.

As Equation 1 shows, increasing the tether stiffness, κ_{tether}, increases the SNR because stiffer molecules are better transducers of mechanical movement, whereas decreasing the temperature, the drag coefficient of the bead, or the measurement bandwidth increases the resolution because reducing these factors decreases the Brownian noise. Despite its thermal origin, decreasing the temperature does little to lower the thermal noise because the biologically permissive temperature range is a small percentage of the absolute temperature. Decreasing bead size improves resolution because smaller beads fluctuate faster than larger beads and thus contribute less Brownian noise on the measurement bandwidth (36, 37).[4] Unfortunately, for technical reasons, it can be difficult to use beads with diameters smaller

[3]This equation is valid for motions slower than the viscous timescale mentioned above. This timescale, set by the ratio of the drag coefficient to the trap stiffness ($\tau = \gamma/\kappa$), provides a fundamental limit to the temporal resolution of an optical tweezers because the trapped bead acts a low-pass filter, averaging faster motions.

[4]Although the total amount of noise over all frequencies is fixed by the equipartition theorem (36, 37), small beads distribute this noise over a wider frequency range, leaving less noise at the low frequencies in which measurements are made.

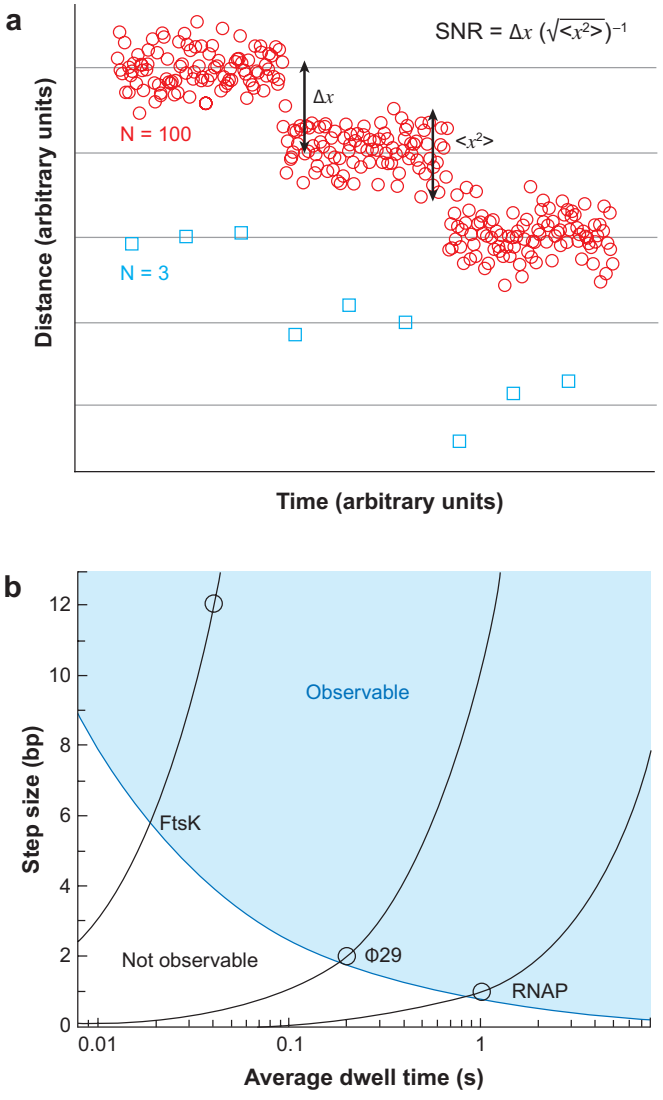

Figure 2

Spatial resolution versus temporal resolution. (*a*) The signal-to-noise ratio (SNR) for a given step is defined as the ratio of the mean distance between steps, Δx, to the noise in a given step $\sqrt{\langle x^2 \rangle}$. The information in the step clearly depends not just on the SNR of the data, both sets of steps pictured here have a SNR of 4, but also on the number of uncorrelated points that make up the step, 100 for the red circles and 3 for the blue squares. (*b*) For a given set of experimental parameters, Equation 2 defines a region of step size and step duration that are observable. Steps that are larger and slower than the solid blue line, for example, could be observed with a two-trap system with equally sized 1-μm beads and a 1-μm long dsDNA molecule held at a tension of 10 pN, assuming that a SNR of 4 and that on average 3 uncorrelated points per step are required for observation. The solid black lines correspond to the possible step sizes and dwell times (using the fact that $\Delta \ell = v\langle \tau \rangle$) that would produce the lowest observed velocity, v, for *Escherichia coli* RNA polymerase (RNAP) (1 bp/s) (58), the bacteriophage φ29 (10 bp/s) (133), or the DNA translocase FtsK (300 bp/s) (52). The circles correspond to the observed (58) or estimated step sizes of these motors (52, 133). Thus, although 1-bp steps could be observed for RNAP, the lowest velocity observed for FtsK would require the steps to be at least ~6 bp in size for the same experimental setup.

than several hundred nanometers (34).[5] Finally, a smaller measurement bandwidth improves resolution because it allows additional averaging of the fluctuations in the signal, although the lowest value of the bandwidth is limited by the speed of the enzyme, as discussed below. Interestingly, there is no dependence in Equation 1 on trap stiffness, despite the fact that beads in stiffer traps fluctuate less. The reason is that beads in stiffer traps are also less sensitive to the motions of the biological system. Remarkably, these two factors exactly cancel when taking the SNR, leading to the finding that trap stiffness has no effect on the Brownian limit to resolution. Because optical tweezers operating in force feedback can be essentially thought of as optical traps with zero stiffness, force feedback does not offer any improvement in this resolution limit.

Are Two Traps Better than One?

An expression similar to the one above has been derived by Moffitt et al. (36) for the two-trap geometry in **Figure 1*c***. It would appear at first glance that the addition of a

[5]The strength of the optical trap, stiffness per power, and the sensitivity of back-focal-plane interferometry both reach a maximum with a bead whose diameter is roughly equal to the wavelength of the trapping light in water and drop off quickly for larger or smaller beads (34).

second bead subject to Brownian fluctuations would increase the total noise in the system. This is true, it turns out, only when the beads are treated independently of each other. In reality, the dynamics of the two beads are correlated because they are tethered together. Recent theoretical work and experimental verification by the authors (36) demonstrate that these correlations can be exploited to minimize the effect of Brownian noise on the spatial resolution of dual-trap systems. This improvement in resolution stems from the fact that fluctuations can be divided into two components: (*a*) symmetric, where the beads move in the same direction, i.e., in phase, maintaining a constant separation, or (*b*) antisymmetric, where they move in opposite directions, i.e., out of phase, stretching or compressing the molecule tethering them. Because the displacements associated with the activity of a biological system alter the extension of the tether, only the antisymmetric component of this noise contributes to limiting resolution. Thus, by monitoring the motion of both beads simultaneously, it is possible to discard the noise caused by symmetric motion with a differential measurement, improving the resolution of the system.

When the motion of both beads is monitored in this differential fashion, the SNR for a dual-trap system takes an identical form to that of Equation 1, but with γ replaced by $\gamma_{eff} = \gamma_1\gamma_2/(\gamma_1 + \gamma_2)$, where $\gamma_{1,2}$ are the drag coefficients of each of the beads (36). Because γ_{eff} is smaller than either $\gamma_{1,2}$, the spatial resolution on a given bandwidth is higher for a system with two optical traps in which the movements of the beads in both traps are monitored than in a system with a single optical trap. Thus, a dual-trap geometry in which the motion of both beads is monitored is the best experimental geometry for limiting the effects of thermal noise (36). Physically, the reason for this improvement is that both beads are involved in the dissipation of thermal energy and thus dissipate this energy more quickly, producing less fluctuation on the measurement bandwidth just as a smaller bead.

What Resolution Has Been Achieved?

The recent advances in instrument stability and measurement, detailed above, have pushed the spatial resolution of optical tweezers to the angstrom scale. With two beads in two optical traps tethered by a single piece of dsDNA as in **Figure 1*c***, stepping movements of only 3.4 Å at 0.5 to 1 s per step can now be detected (34, 36, 58). With this resolution Abbondanzieri et al. (58) were able to measure the single base pair motions of *Escherichia coli* RNA polymerase (RNAP) when slowed to ~1 nucleotide/s with low nucleotide concentration under assisting forces as low as 18 pN. In these experiments, one of the two traps was much stiffer than the other so that the motions of the bead in the stiffer trap could be ignored. Moffitt et al. (36) demonstrated that by forming two optical traps of comparable stiffness and by monitoring the motion of both beads, as discussed above, it is possible to obtain similar resolution even when using larger beads and when applying several times lower tension on the DNA tether.

What Is Needed to Observe Steps?

The measurement bandwidth, B, is a convenient unit from an instrumentation perspective because it characterizes the rate at which data are collected and averaged; however, for the purpose of studying periodic biological processes, such as the stepping of a molecular motor, the average period of the system (the time per step of a molecular motor, for example) $\langle\tau\rangle$ is a much more intuitive quantity. The bandwidth of the measurement can be related to this quantity by $2B = N/\langle\tau\rangle$, where N is the number of uncorrelated measurements per average dwell.[6] $N \geq 1$ sets the limit on the measurement bandwidth if one does not wish to average over the individual

[6]The factor of two originates in the subtle difference between the bandwidth of the measurement and the frequency at which the data are sampled, namely, $f_{samp} = 2B$.

periods of the system. Using this expression it is possible to show that the observation of a step of size $\Delta\ell$ with an average dwell time of $\langle\tau\rangle$ requires that

$$\Delta\ell\sqrt{\langle\tau\rangle} \geq \frac{\sqrt{2k_BTN\gamma}}{\kappa_{tether}} SNR. \qquad 2.$$

This relationship makes explicit the inverse relationship between spatial and temporal resolution. Observation of single base pair steps at 1 step per second is just as difficult as observing steps of two base pairs at 0.25 s per step or steps of 10 bp at 10 ms per step. **Figure 2*b*** further illustrates this point.

Although Equation 2 provides a more intuitive connection to the physical motions of the biological system, it does not determine what SNR or what value of N are required for the observation of steps and the extraction of unbiased kinetic information from these steps. Recent empirical work was aimed at addressing these questions. For example, one recent study (59) has suggested that a SNR of 4 or better is required for the measurement of step sizes given the most commonly used algorithm, the pairwise distribution. From other work, a value of $N \approx 1$ appears to be sufficient for the measurement of steps (34, 36, 58), although little is reported on how this affects the determination of the dwell times of steps. Similar results have been obtained for some of the more sophisticated step-finding algorithms (60–63). The empirical approaches of these studies provide useful rules of thumb for designing experiments, but a systematic theoretical study of the affect of SNR and N on step size and dwell time measurements is still needed.

What about Accuracy?

An underappreciated effort that has been occurring in parallel to the development of high-resolution trapping techniques has been the continued improvements in the accuracy of their calibration. The degree of accuracy—the relative error between the measured value and actual value—needed in a given experiment depends on the particular application. For instance, a 10% calibration error might be tolerated in the measurement of RNAP steps; a measurement of a 1.1-bp step size would not be interpreted as inconsistent with a 1-bp step. In contrast, FtsK has been estimated to step in increments of 12 bp (52); direct observations of these steps, with ~10% calibration error revealing an 11-bp step size, would impact how the data are interpreted and how models of the motor operation are constructed. More importantly, although it is widely believed that nucleic acid translocases move in discrete increments that are integer multiples of a single base pair, this need not be true. High-resolution optical tweezers have the potential to test this long-standing paradigm through direct observations, but only if the accuracy of these measurements is high. Thus, if models are to be constructed faithfully and without bias, efforts to improve the accuracy of optical tweezers measurements must go hand in hand with efforts to improve resolution. Recent advances in this direction have focused on developing new calibration techniques (64) and reducing systematic errors in existing calibration procedures (54, 65, 66). Though the nature of these developments is too technical to warrant detailed discussion in this review, they are an important contribution to the field, and the interested reader is encouraged to read the literature describing these advances (54, 64).

Pairwise distribution: a histogram of the distances between every two points in the trajectory of a molecular motor

HYBRID AND NOVEL INSTRUMENTS

In parallel to the advances in high-resolution optical trapping, the field has also seen the development of novel and hybrid optical tweezers. These instruments significantly expand the capabilities of the traditional optical tweezers, allowing the manipulation of more complicated biological systems, the control of additional variables such as torque, or the simultaneous use of additional forms of single-molecule manipulation and detection. In this section, we review these recent advances.

Why Create Hybrid and Novel Instruments?

Time sharing: a process that rapidly switches a single laser between multiple locations to form multiple optical traps

Acousto-optic deflector (AOD): a crystal that acts as a tunable diffraction grating under the application of radiofrequency sound waves

The motion of many molecular motors is inherently three-dimensional, involving not only translocation along a molecular track, but movements in orthogonal directions and even rotation around this track. Moreover, this motion may involve many simultaneous conformational changes within the protein. Traditional optical tweezers, which typically project all motion onto a single axis, are not good tools for the investigation of these additional motions. Furthermore, inside the cell, molecular motors do not work in isolation but are part of large complexes that involve the tightly coordinated interaction of multiple molecules at multiple locations. Again, traditional optical tweezers, which can manipulate only a limited number of molecules with one or two optical traps, are poorly suited to recreate this aspect of the cellular environment. Both of these limitations may be overcome by introducing new manipulation and measurement capabilities into the standard optical tweezers assay.

Why Manipulate More than One Molecule?

To illustrate one method in which novel forms of manipulation have been integrated into optical tweezers, consider the technical problems associated with using optical tweezers to study the condensation of the bacterial chromosome. The bacterial chromosome, and all of its associated condensing proteins, is a complex, dynamic structure whose integrity and degree of condensation involves interactions between many distal regions of DNA and the participation of many proteins. Among these proteins is the nucleoid structuring protein H-NS, a dimeric protein that has two independent DNA-binding domains (67). The orientation and mode of binding of these domains—whether they bind adjacently to the same DNA segment or bridge distal segments, forming loops—and thus their role in the condensation of the bacterial chromosome were not known (67). To complicate matters, initial single-molecule studies using only a single piece of DNA revealed that H-NS did not compact a single DNA molecule but rather extended it (68, 69).

To address this problem, Dame et al. (70) constructed an optical tweezers with four independently controllable optical traps, which they term the Quad-trap (**Figure 3*a***). With this geometry it was possible for the authors to individually trap four polystyrene beads and use them to manipulate two independent DNA molecules. With this ability, the authors were able to determine that H-NS can only bridge DNA strands when they are overlapping before incubation with H-NS but not when they are coated with H-NS and then overlapped. This observation suggests that a single H-NS dimer bridges and condenses distal regions of the chromosome by DNA-protein-DNA interactions as in **Figure 3*a***. These authors were also able to measure the force needed to both unzip and shear a DNA-H-NS-DNA assembly, and because they designed their instrument to maintain the high spatial and temporal resolution of traditional optical tweezers, they observed the discrete steps in which the condensed DNA unzipped. The use of four optical traps allowed these experiments to be conducted in a straightforward and simple fashion not possible with only one or two optical traps.

How Do You Create Novel Optical Potentials?

The four traps in the Quad-trap instrument used by Dame et al. (70) are formed by splitting a single laser via polarization, using one polarization to form one of the optical traps, and then time sharing the other polarization with an acousto-optic deflector (AOD) to form the other three traps (70) (**Figure 3*b***). Time sharing a single laser between multiple optical traps is possible as long as the laser is returned to the same location faster than the

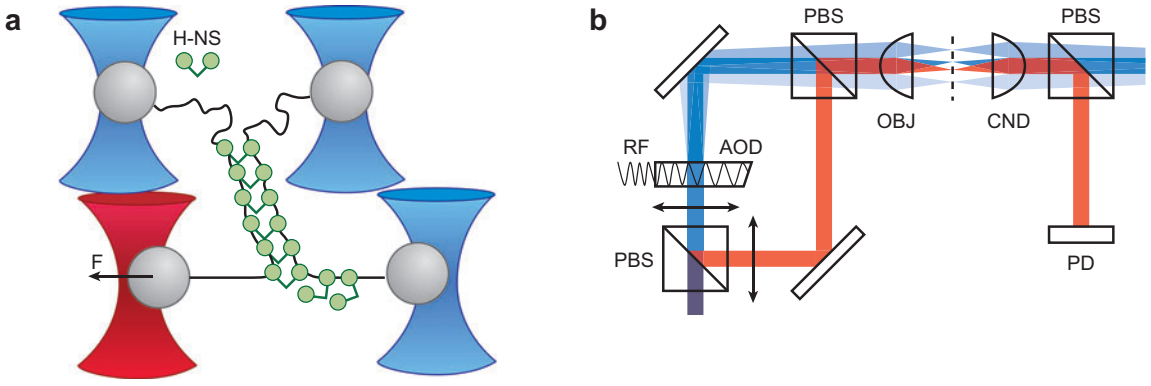

Figure 3

Control of multimolecular complexes with multiplexed optical tweezers. (*a*) The formation of four optical traps allows control of a DNA-H-NS-DNA complex not possible with only a single piece of DNA. By measuring force with one of the optical traps (*red*), it is possible to follow the unzipping of this complex on the nanometer scale. (*b*) The formation of four optical traps is accomplished with an acousto-optic deflector (AOD). When driven by different radio frequencies (RFs), this device rapidly shares one of the polarizations of the laser (*blue*), split with a polarizing beam splitter (PBS), between three different traps. The other polarization (*red*) is not shared, allowing light from this trap to be easily separated with another PBS after the traps are formed with a high-numerical objective (OBJ), and the scattered light is collected with a condenser (CND). Projecting this light onto a position sensitive photodector (PD) allows precise measurement of the response of the bead in the trap that is not time shared. Note that this is a schematic diagram only, necessary relay lenses have been left out for clarity (70).

time it takes for the bead to diffuse away from that location, typically on the order of tens of milliseconds. For simplicity, Dame et al. detect the force only in the single trap that is not time shared (**Figure 3*b***), although Guilford et al. (71) have shown it is possible to perform the complicated signal processing necessary to extract the force and position of each of the beads in multiplexed optical traps.

Time-sharing techniques using AODs and other methods have been described previously (30, 71–73) and have been used to generate multiple optical traps for the study of nonprocessive motors such as myosin (74). Furthermore, it is possible to use this technique to generate novel optical potentials in addition to multiple optical traps. If the physical location of the time-shared traps are within the diameter of the trapped bead, and if the trap is shifted fast enough, the bead observes an average two-dimensional potential that can be arbitrarily shaped given the average duration and light intensity of the trap at each location. Such novel optical potentials have been used to form regions of constant force for the study of the dynamics of DNA relaxation (75), and also so-called keyhole traps (76), potentials that are capable of trapping a bead bound to a cytoskeletal filament while also aligning the filament within the trap. These potentials have been useful for the study of the forces involved in the dynamics of microtubule and actin filament assembly (60, 76, 77).

Another powerful approach to create multiple optical traps or novel optical potentials is to use spatial light modulators to imprint a phase image of the desired traps in the trapping light, which is then transformed by the objective into the desired location and number of optical traps.[7] Such holographic optical tweezers offer enormous versatility in the number, size, shape, and three-dimensional position of these traps and have thus inspired

Spatial light modulator: this device allows precise, dynamic control over the phase and intensity of different regions of an incident laser

[7]Lenses also work by modifying the phase of different regions of the incoming light; thus, spatial light modulators can be thought of as computer-controlled lenses of arbitrary shape.

a large body of research and development (for brief reviews see References 78 and 79). Unfortunately, there is currently no method for detecting the force and response on the trapped beads that rivals the resolution and bandwidth offered by back-focal plane interferometry or comparable laser detection methods. The problem is inherent in the use of phase to encode the individual optical traps. Because the phase of the light is also changed upon scattering from the bead, it is difficult to discriminate and separate the scattered light from each of the individual trapped particles. One possible solution is to follow Dame et al. (70) by introducing an additional optical trap formed from a unique polarization or wavelength to measure force and use the holographic optical tweezers for manipulation only. Alternatively, the additional laser need not be powerful enough to form an optical trap but could simply be a detection laser (30). Such a design would provide greater versatility, allowing the force and position of any of the optically trapped beads to be monitored.

Why Add Torque to an Optical Tweezer?

Not all hybrid instruments that involve new forms of manipulation have focused on the assembly and manipulation of complex biological systems. For example, much effort has been dedicated to extending optical tweezers to the measurement of additional degrees of freedom, such as rotation. These new instruments offer the potential for studying biological motors that generate twist and torque in conjunction with force. In addition to the more obvious examples, such as the flagellar motor (80), F_1F_0 ATP synthase (81, 82), and type II topoisomerases (83–85), many canonically linear motors are also believed to produce rotation. For example, motors such as DNAPs and RNAPs, which involve the synthesis of a nucleic acid chain from a DNA template, most likely follow the helical pitch of this template, generating a relative rotation of one turn for every 10.5 bp translocated. Moreover, the mechanisms of multimeric, ring-shaped nucleid acid motors may also involve rotation. In the chromosome segregation DNA translocase FtsK (86), or the viral DNA-packaging motor of bacteriophage φ29 (87), the symmetry mismatch between the multimeric ring of the motor and that of the DNA helix suggests that motor and DNA twist relative to each other to maintain specific contacts during translocation. Thus, measurements of the twist per distance translocated can provide insight into the number of subunits within the motor, the types of contacts these subunits make with the track, and even the spatial order in which the subunits make these contacts during translocation. Given these considerations, it is of great interest to find methods to control twist and measure torque while simultaneously measuring linear motion and force with the resolution of traditional optical tweezers.

How Do You Add Rotational Control to Optical Tweezers?

Bryant et al. (88) introduced one of the first methods for providing controlled rotation into an optical tweezers. By adding a rotating micropipette (**Figure 4*a***), the authors were able to induce twist on a molecule (88) or molecules of DNA (89) while simultaneously measuring force and extension of the molecule. Although this method of adding twist is relatively simple and need not involve extensive modification to an existing instrument, it does not provide a direct measurement of torque. The authors solved this problem by adding a small "rotor" bead to the side of the DNA. The engineering of a nick on one strand of the DNA near this rotor bead allowed the single bonds of the opposite strand to act as molecular swivels. It turns out that the angular velocity of this bead—driven by the torque on the DNA and balanced by the torque generated by viscous drag—is directly proportional to the torque stored on the DNA. By over- or undertwisting the DNA and then watching the rate at which the

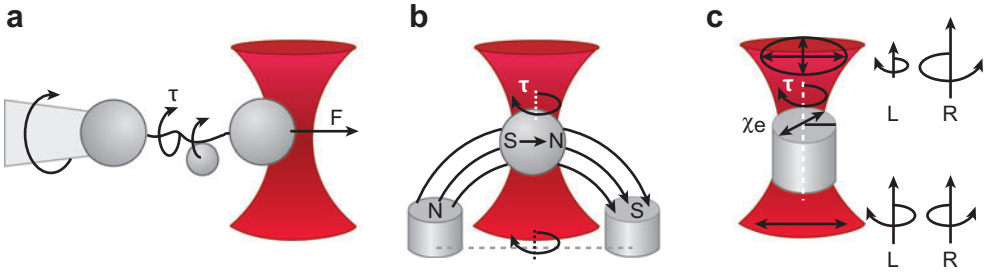

Figure 4

Methods for generating torque in optical tweezers. (*a*) Rotation of a micropipette allows the addition of twist to a single molecule of DNA and the application of a torque, τ, which is measured by the rotation of a small "rotor" bead attached to the DNA. (*b*) Optically trapped paramagnetic beads develop a magnetic dipole in the presence of a magnetic field, which can be used to rotate the bead by rotating the magnetic field. (*c*) Optically trapped birefrigent particles, such as quartz microcylinders, change the polarization of the trapping light, generating an angular momentum change, and, thus, a torque if the extraordinary axis (χ_e) of the particle is rotated with respect to the incident polarization. If linearly polarized trapping light is used (with no net angular momentum owing to the equal parts left (L) and right (R) of circularly polarized light), the optical torque can be measured directly by determining the amount of right and left circularly polarized light in the forward-scattered light (102, 103).

rotor bead dissipated this torque, the authors were able to determine the constant of proportionality between the twist applied to the molecule and the torque stored—the torsional rigidity of the molecule (88). Moreover, the researchers were able to use this experimental setup to probe the detailed phase diagram of dsDNA, determining the forces and torques at which it undergoes transitions between different structural forms (88). By introducing a second DNA molecule and using the rotating micropipette to braid these molecules, Stone et al. (89) were able to also use a rotating micropipette to study the mechanism of type II topoisomerases.

Instead of introducing a rotating micropipette, which may not be practical in all optical setups, it is also possible to trap a paramagnetic bead and use external magnets to rotate this bead in the optical trap (90–92) (**Figure 4*b***). The addition of magnets to a standard optical tweezers can be relatively simple and provides a straightforward method for adding the ability to twist biomolecules to a preexisting instrument. Unfortunately, there is again no direct method for measuring the torque on the paramagnetic bead. As before, it is possible to introduce a small rotor bead to measure the torque on DNA; however, because the magnetic bead is free to rotate in the optical trap, it is also possible to track its rotation, assuming the bead is visibly asymmetric (91). By monitoring the phase delay between the rotation angle of this defect and that of a rotating magnetic field caused by the viscous drag on the rotating bead, it is possible to calibrate the torque for each bead (91). The potential drawbacks of such a method are that it must be repeated for each trapped bead and requires sensitive measure of the relative angle between the bead defect and the magnetic field. Recently, Crut et al. (93) used such magneto-optical tweezers to measure the relaxation of plectonemic DNA.

A more instrumentally challenging, but more powerful, method for introducing torque-generating capabilities into optical tweezers is to use the angular momentum carried by light. Torque may be generated on the trapped particle either by transfer of this angular momentum to the particle via partial absorption of the trapping light (94–96) or by addition of angular momentum into the trapping light by the trapping particle itself (97, 98). In the latter case, the asymmetry of the particle, either because of its shape

Birefringence: an optical asymmetry in which light of different polarization travels at different speeds through a material

Extraordinary axis: a birefringent crystal axis that allows light to travel fastest when its polarization is aligned with this axis

(99–101) or its birefringent properties (97, 98, 102), changes the angular momentum of the incoming beam, producing a torque on the particle to conserve angular momentum. The benefit of such a method is that it does not require the absorption of trapping light, allowing the use of relatively transparent particles, which in turn reduces the effect of laser heating (97). Furthermore, if the angular momentum is transferred into the polarization of the light, as opposed to the spatial distribution of the light, then it is possible to measure exactly the torque on the particle via changes in the polarization state of the scattered light (102, 103). Specifically, if trapping is accomplished with linearly polarized light, which carries no net angular momentum, the torque on the particle can be measured by determining the excess of right-circularly to left-circularly polarized light after its interaction with the trapped particle (**Figure 4*c***). In direct analogy to force and position, optical measurement of torque and rotation of the linear polarization of light can be done with very high bandwidth, making it possible to create torque feedback systems that rotate the polarization of the trapping light dynamically to keep the applied torque on the system constant (102). For a comprehensive review on optical torque see Reference 104.

One potential drawback of such optical torque wrenches is the need for uniform birefringent particles that have the extraordinary axis oriented correctly with the desired axis of the experiment and with any asymmetries within the trapping particle (98). Recently, Deufel et al. (105) have demonstrated a powerful solution to this problem by fabricating micron-sized quartz cylinders with the extraordinary axis of the quartz uniformly aligned along the short axis of the cylinder. The cylindrical shape ensures that the long axis will align in the axial direction of the optical trap and properly orient the extraordinary axis of the cylinder with the trapping polarization (105). Furthermore, the authors amino-functionalize only one surface of the cylinder, controlling the attachment point of the biological system and further ensuring that rotation occurs around the correct axis. The power of their experimental setup was demonstrated by measuring simultaneously the torque on and the extension of a single piece of dsDNA while twisting the molecule under a constant optical force. In this simple proof-of-principle experiment (105), several of the mechanical features of dsDNA were measured simultaneously, such as the twist stretch coupling (106, 107), the torsional rigidity (88), and the critical torque for the phase transition between B-form DNA and supercoiled DNA (88).

Finally, it is also possible to introduce twist or apply torque to a biological system with a fixed axis by simply moving an optical trap in a circle around the fixed axis of the sample. Pilizota et al. (108) have constructed an optical tweezers with this capability for the study of the bacterial flagellar motor. Because the radius of the circle ascribed by the motion of the optical tweezers is known, it should be possible to calculate the applied torque from the applied optical force. For systems in which there is no simple fixed axis, one may use a second optical trap to form this rotation point (109).

What Other forms of Manipulation Can Be Integrated with Optical Tweezers?

In the above examples, it is the bead in the optical trap that is subjected to some additional form of manipulation; however, there have been several recent examples of employing optical tweezers to measure the response of other manipulation techniques. For example, Keyser et al. (110, 111) recently integrated optical tweezers with nanopores and demonstrated that it is possible to pull on a single piece of DNA partially threaded through a nanopore and driven by an applied electric field, a feat recently repeated by Trepagnier et al. (112). By measuring the required force as a function of the voltage across the nanopore, Keyser et al. were able to measure the

effective free charge per base pair of DNA (111). In addition, Huisstede et al. (113) integrated a glass micropipette scanning probe in a single-trap optical tweezers. They demonstrated that by correlating the response of the bead in the optical trap to the position of a scanning probe coated with antibodies to digoxigenin, it was possible to localize individual digoxigenin modifications on a single piece of DNA.

How is Single-Molecule Fluorescence Used?

The field of fluorescence detection is based on the ability to optically excite small fluorophores, small organic molecules or proteins, or semiconductors nanocrystals, i.e., quantum dots, which emit photons of a longer wavelength when they relax back to their ground state. One of the major benefits of this technique is that the system is largely noninvasive: Typical fluorophores are small, and the excitation and detection are completely optical, allowing far-field excitation and imaging. Furthermore, there are a wide range of methods for illuminating the sample: epi-illumination in which the entire sample plane is bathed in the excitation light, confocal illumination in which a small diffraction-limited spot is excited, or total internal reflection where an evanescent wave is used to excite a small region near the surface of the sample slide. Useful single-molecule measurements can be made with large numbers of dyes, through multiply labeled molecules, or through only a few dyes. In the case of small numbers of dyes, photophysical interactions between the dyes such as Förster resonant energy transfer (FRET) or self-quenching can be used to probe small distance changes or can serve as molecular on-off switches. Additionally, with advances in single-fluorophore imaging, it is possible to track single dyes on the nanometer and millisecond scales. For reviews of the application of single-molecule fluorescence see References 21, 45, 114, and 115.

How Do You Use Fluorescence to Visualize Molecules in Optical Tweezers?

FRET: Förster resonant energy transfer

Fluorescence as a method for visualizing single molecules has been utilized since the very first experiments that manipulated DNA (116). In the first optical tweezers assay, a long piece of DNA (tens of microns) was labeled with ethidium bromide and stretched between two beads held in two optical traps (117). The relaxation of the DNA as one bead was released could be followed by simply watching the movements of the fluorescently labeled DNA. Similar assays have been used to not only study the polymer physics of DNA (118, 119), but have also been adapted to the study of molecular motors, such as the helicase complex RecBCD (120–122). Controlled fluid flow was used to extend the DNA, and changes in its length visualized by fluorescence microscopy revealed the progress of the motor. Although such assays are powerful, the optical trap is used only as a means of manipulating the DNA and holding it stationary against a fluid flow.

In one recent example, which illustrates the possibilities of combining fluorescence imaging of multiply labeled molecules with force measuring optical tweezers, the elastic properties of a single piece of dsDNA heterogeneously coated with filaments of Rad51, an important component in eukaryotic homologous recombination, were investigated (123). In this assay, fluorescently labeled Rad51 filaments could be imaged on a piece of dsDNA tethered between two optically trapped beads (**Figure 5*a***). The response of both the fluorescent filaments and the bare DNA to an applied load could be followed simultaneously with fluorescence microscopy and the deflection of the trapped beads, allowing the authors to dissect the elastic properties of each component from a measurement of the heterogeneous system (123). This example illustrates one application of combined optical tweezers-fluorescence measurements: the ability to demarcate different parts of a larger molecular

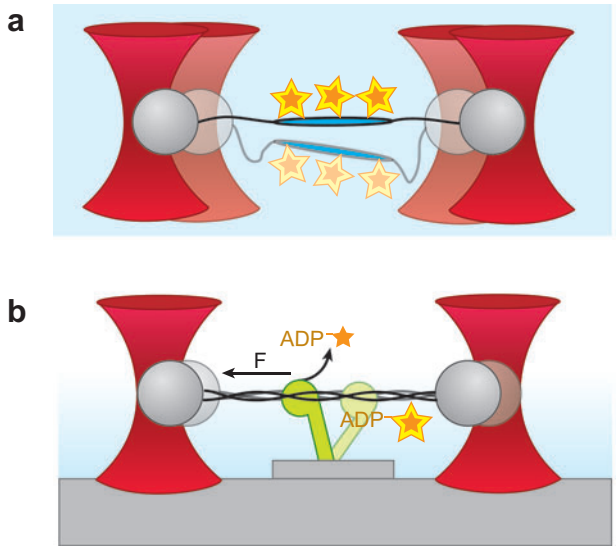

Figure 5

Fluorescence in optical tweezers. (*a*) Multiple fluorophores (*stars*) can be used to tag different regions of a heterogeneous biological tether allowing the individual response of each section of the tether to optical forces to be probed with video microscopy. (*b*) Single fluorescently labeled molecules can be used to correlate the bound nucleotide state and the force-generating transition of a molecular motor such as myosin. Total internal reflection illumination limits the spatial extent of the excitation light (*blue*), lowering the fluorescent background from free nucleotides (124).

complex and measure the response of each to an applied load.

Can You Use Single Fluorophores with Optical Tweezers?

Although the use of multiple fluorophores to label single molecules offers many advantages, there are many applications of fluorescence imaging that require the use of only one or two dyes. The earliest example of single-molecule fluorescence combined with optical tweezers is still perhaps one of the most impressive accomplishments in the field. Ishijima et al. (124) suspended an actin fiber between two optical traps and measured the deflection of the fiber by individual myosin heads. However, the true *tour de force* of this experiment was in the incorporation of total internal reflection fluorescence excitation and single-fluorophore detection into this system, which allowed the investigators to simultaneously detect single fluorescently labeled ATP (ATP-Cy3) bind to the myosin (124). This experiment made it possible to directly correlate the nucleotide binding state of the motor and its power stroke (**Figure 5*b***). The authors confirmed that binding of nucleotide occurred simultaneously with the disengagement of myosin from actin and that, rather controversially (125), the power stroke of the motor did not correspond to the release of ADP but was a different and subsequent kinetic transition (124).

The widespread use of single-molecule fluorescence measurements and optical tweezers force and displacement measurements has been slowed, however, owing to several technical problems. The main difficulty is that the lifetime of the fluorescent dyes decreases dramatically because of the absorption of a near-infrared trapping photon by the fluorescent excited state (126). This effect was not experienced in the study just described, as the rigidity of actin allowed the investigators to use long filaments and thus separate the region in which single fluorophores were imaged and the locations of the optical traps by ~10 μm. Unfortunately, the detection of molecular motions is greatly inhibited by more flexible polymers, such as dsDNA, of this length because the stiffness of the tether decreases with increased length and lower stiffness degrades resolution, as explained above. Nevertheless, it is possible to still measure and apply force with the optical trap on long pieces of DNA and then use fluorescence changes owing to FRET, for example, as a sensitive measure of distance (126a). In applications requiring close proximity between the optical trap and the fluorescent dyes, this effect on lifetime can be mitigated somewhat by introducing antioxidants (126), judicious choice of dye (the fluorophore Cy3 is more sensitive to this effect than TMR or Alexa555, for example) (127, 128), or even using orthogonal polarizations for the

trapping light and the fluorescence excitation (126). An alternative method is to avoid simultaneous exposure of the fluorophores to both light sources simultaneously. Brau et al. (129) have developed a method in which they interlace the excitation light and the trapping light, with no deleterious effects on trapping or fluorescence as long as the modulation rate is high enough. They have accomplished a 20-fold improvement in the lifetime of Cy3 molecules and have demonstrated the principle of their method by simultaneously detecting conformational changes in DNA hairpins under load using single fluorophores (129) and FRET (130).

CONCLUSIONS AND PERSPECTIVES

As described in this review, optical trapping techniques have rapidly advanced in recent years along two fronts: the improvement of spatial resolution and accuracy, and the hybridization of techniques for the simultaneous measurement of multiple observables. The former developments have been motivated by the desire to understand conformational changes in proteins and nucleic acids at their most fundamental spatial and temporal scales. High-resolution optical tweezers can now directly detect these motions, together with the actual stepping of a number of molecular motors and the conformational changes resulting from the mechanical unfolding of proteins and nucleic acids. More importantly, the improved spatial and temporal resolution make it now possible to study a much larger class of biological processes that occur at these length scales, a regime traditionally accessible only to high-resolution structural methods. For example, conformational changes that lie at the heart of many cellular processes, such as enzyme catalysis, cell signaling, and ion channel gating, all involve motions of protein domains at the angstrom scale and therefore internal generation of force (17). The ability to resolve slow motions on this spatial scale should thus allow the direct study of these motions and the effect of force on their kinetics. This development thus provides the exciting prospect of complementing the static pictures provided by atomic structures with kinetic measurements of conformational changes on similar length scales.

In spite of these recent advances in resolution, there is still much room for improvement. All high-resolution instrumentation studies report that experimental noise becomes limiting at longer timescales, typically one second or longer (34, 36, 58). Although the source of this noise remains in some cases unclear, its elimination will be essential to achieve even higher spatial resolution on those slow time regimes. The extension of angstrom resolution to faster timescales is certainly possible as well, as Equations 1 and 2 demonstrate. However, this next leap in resolution will most likely require more radical ideas and perhaps novel experimental geometries to allow manipulation of shorter and stiffer tethers and smaller beads.

The second trend in the advancement of optical tweezers has been to extend the technique to the study of increasingly complex systems to better duplicate their in vivo physiology. The development of hybrid techniques has aimed to address the challenge of probing these complex macromolecular assemblies. Although the measurement of displacement and force along one axis afforded by traditional optical tweezers has proven insufficient to fully characterize the dynamics of some systems, hybrid methods provide the opportunity for additional readouts such as force and displacement along complementary axes, torque, and angle, or fluorescence position and orientation. These capabilities should allow one to measure the generation of force and torque simultaneously on many molecular motors. Moreover, not only will it be possible to correlate nucleotide state with motor translocation, as Ishijima et al. (124) did with myosin and single-fluorophore

detection of labeled nucleotides, but it may also be feasible to use optical techniques to control the nucleotide state as well, with caged-ATP molecules, for instance, or more exotic photoswitchable molecules (131, 132). Finally, in the future we expect hybrid techniques to unleash the full arsenal of single-fluorophore imaging methodologies (115).

Many of the techniques described in this review have still only had proof-of-principle demonstrations, in part, because they are so new, but also because the instrumentation involved is relatively complex. Nevertheless, these techniques hold great promise to address many fundamental problems in biology at the single-molecule level. The next step in the development of optical tweezers instruments will no doubt combine these hybrid techniques with the highest spatial and temporal resolution. Although most likely very difficult to construct, these instruments promise an unprecedented amount of information. Imagine following the discrete steps of a molecular motor at high resolution while correlating these steps with domain motions revealed by single-molecule fluorescence. Almost 35 years ago Arthur Ashkin was experimenting with intense light and latex beads suspended in water, a work that spawned this field (1). Today, as the field matures and important technical advances continue to be made, it is clear that optical tweezers will increasingly become an important weapon in the full arsenal of the biochemist.

SUMMARY POINTS

1. Optical tweezers have seen several exciting technological advances in the past years, which will allow researchers to dissect the molecular mechanism of more complicated biological systems in greater detail.
2. By addressing both experimenal and Brownian sources of noise, it is now possible to resolve angstrom scale motions on the second timescale.
3. The use of multiple optical traps or novel optical potentials is allowing researchers to manipulate biological systems of greater complexity.
4. Several methods have been demonstrated for introducing the capability of applying and measuring torque simultaneously with force in optical tweezers.
5. Many of the initial hurdles in combining optical tweezers and single-molecule fluorescence have been overcome, and these hybrid instruments promise to provide an unprecedented level of detail into the inner workings of molecular motors.

FUTURE ISSUES

1. Further improvement in the resolution of optical tweezers is possible but will require greater attention to experimental sources of noise and the use of smaller beads and shorter tethers.
2. Because of the relatively uninvasive nature of optical tweezers, it should be possible to integrate this technique with other forms of single-molecule manipulation and measurement.
3. The full power of the myriad hybrid techniques now awaits application to a wide range of biological systems.

DISCLOSURE STATEMENT

The authors are not aware of any biases that might be perceived as affecting the objectivity of this review.

ACKNOWLEDGMENTS

We thank M. Nollmann, C.L. Hetherington, and W. Cheng for a critical reading of the manuscript. J.R.M. acknowledges the National Science Foundation's Graduate Research Fellowship and Y.R.C. the Burroughs Welcome Fund's Career Awards at the Scientific Interface for funding.

LITERATURE CITED

1. Ashkin A. 1970. *Phys. Rev. Lett.* 24:156–9
2. **Ashkin A, Dziedzic JM, Bjorkholm JE, Chu S. 1986. *Opt. Lett.* 11:288–90**
3. MacDonald MP, Spalding GC, Dholakia K. 2003. *Nature* 426:421–24
4. Pauzauskie PJ, Radenovic A, Trepagnier E, Shroff H, Yang P, Liphardt J. 2006. *Nat. Mater.* 5:97–101
5. Agarwal R, Ladavac K, Roichman Y, Yu GH, Lieber CM, Grier DG. 2005. *Opt. Express* 13:8906–12
6. Furst EM. 2005. *Curr. Opin. Colloid Interface Sci.* 10:79–86
7. Meiners JC, Quake SR. 1999. *Phys. Rev. Lett.* 82:2211–14
8. Henderson S, Mitchell S, Bartlett P. 2001. *Phys. Rev. E* 64:061403
9. Henderson S, Mitchell S, Bartlett P. 2002. *Phys. Rev. Lett.* 88:088302
10. Hough LA, Ou-Yang HD. 2002. *Phys. Rev. E* 65:021906
11. Liphardt J, Dumont S, Smith SB, Tinoco I Jr, Bustamante C. 2002. *Science* 296:1832–35
12. Wang GM, Sevick EM, Mittag E, Searles DJ, Evans DJ. 2002. *Phys. Rev. Lett.* 89:050601
13. Trepagnier EH, Jarzynski C, Ritort F, Crooks GE, Bustamante CJ, Liphardt J. 2004. *Proc. Natl. Acad. Sci. USA* 101:15038–41
14. Collin D, Ritort F, Jarzynski C, Smith SB, Tinoco I, Bustamante C. 2005. *Nature* 437:231–34
15. Bustamante C. 2005. *Q. Rev. Biophys.* 38:291–301
16. Bustamante C, Liphardt J, Ritort F. 2005. *Phys. Today* 58:43–48
17. **Bustamante C, Chemla YR, Forde NR, Izhaky D. 2004. *Annu. Rev. Biochem.* 73:705–48**
18. **Neuman KC, Block SM. 2004. *Rev. Sci. Instrum.* 75:2787–809**
19. Bustamante C, Macosko JC, Wuite GJ. 2000. *Nat. Rev. Mol. Cell Biol.* 1:130–36
20. Bustamante C, Bryant Z, Smith SB. 2003. *Nature* 421:423–27
21. Greenleaf WJ, Woodside MT, Block SM. 2007. *Annu. Rev. Biophys. Biomol. Struct.* 36:171–90
22. Svoboda K, Schmidt CF, Schnapp BJ, Block SM. 1993. *Nature* 365:721–27
23. Finer JT, Simmons RM, Spudich JA. 1994. *Nature* 368:113–19
24. Mehta AD, Rief M, Spudich JA, Smith DA, Simmons RM. 1999. *Science* 283:1689–95
25. Liphardt J, Onoa B, Smith SB, Tinoco I Jr, Bustamante C. 2001. *Science* 292:733–37
26. Zhuang X. 2005. *Annu. Rev. Biophys. Biomol. Struct.* 34:399–414
27. Tinoco I, Li PTX, Bustamante C. 2006. *Q. Rev. Biophys.* 39:325–60
28. Cecconi C, Shank EA, Bustamante C, Marqusee S. 2005. *Science* 309:2057–60

First demonstration of stable optical trapping of micron-sized dielectric objects in three dimensions using a single-beam gradient optical trap.

A detailed review of the myriad mechanical processes in biochemistry.

A comprehensive review of the theory of optical trapping and the practical concerns associated with constructing an optical tweezers.

29. Smith DE, Tans SJ, Smith SB, Grimes S, Anderson DL, Bustamante C. 2001. *Nature* 413:748–52
30. Visscher K, Gross SP, Block SM. 1996. *IEEE J. Sel. Top. Quantum Electron.* 2:1066–76
31. Allersma MW, Gittes F, deCastro MJ, Stewart RJ, Schmidt CF. 1998. *Biophys. J.* 74:1074–85
32. Gittes F, Schmidt CF. 1998. *Opt. Lett.* 23:7–9
33. Pralle A, Prummer M, Florin EL, Stelzer EHK, Horber JKH. 1999. *Microsc. Res. Tech.* 44:378–86
34. Bustamante C, Chemla YR, Moffitt JR. 2008. In *Single-Molecule Techniques: A Laboratory Manual*, ed. PR Selvin, T Ha, pp. 297–324. Cold Spring Harbor, NY: Cold Spring Harb. Lab.
35. Smith SB, Cui Y, Bustamante C. 2003. *Methods Enzymol.* 361:134–62
36. Moffitt JR, Chemla YR, Izhaky D, Bustamante C. 2006. *Proc. Natl. Acad. Sci. USA* 103:9006–11
37. Gittes F, Schmidt CF. 1998. *Eur. Biophys. J.* 27:75–81
38. Visscher K, Block SM. 1998. *Methods Enzymol.* 298:460–89
39. Greenleaf WJ, Woodside MT, Abbondanzieri EA, Block SM. 2005. *Phys. Rev. Lett.* 95:208102
40. Svoboda K, Block SM. 1994. *Annu. Rev. Biophys. Biomol. Struct.* 23:247–85
41. Ashkin A. 1997. *Proc. Natl. Acad. Sci. USA* 94:4853–60
42. Mehta AD, Rief M, Spudich JA. 1999. *J. Biol. Chem.* 274:14517–20
43. Hormeno S, Arias-Gonzalez JR. 2006. *Biol. Cell* 98:679–95
44. Ritort F. 2006. *J. Phys. Condens. Matter* 18:R531–83
45. Cornish PV, Ha T. 2007. *ACS Chem. Biol.* 2:53–61
46. Neuman KC, Lionnet T, Allemand JF. 2007. *Annu. Rev. Mater. Res.* 37:33–67
47. Bustamante C, Keller D, Oster G. 2001. *Acc. Chem. Res.* 34:412–20
48. Kolomeisky AB, Fisher ME. 2007. *Annu. Rev. Phys. Chem.* 58:675–95
49. Schnitzer MJ, Block SM. 1995. *Cold Spring Harb. Symp. Quant. Biol.* 60:793–802
50. Shaevitz JW, Block SM, Schnitzer MJ. 2005. *Biophys. J.* 89:2277–85
51. Asbury CL, Fehr AN, Block SM. 2003. *Science* 302:2130–34
52. Saleh OA, Perals C, Barre FX, Allemand JF. 2004. *EMBO J.* 23:2430–39
53. Pease PJ, Levy O, Cost GJ, Gore J, Ptacin JL, et al. 2005. *Science* 307:586–90
54. Berg-Sorensen K, Flyvbjerg H. 2004. *Rev. Sci. Instrum.* 75:594–612
55. Nugent-Glandorf L, Perkins TT. 2004. *Opt. Lett.* 29:2611–13
56. Carter AR, King GM, Ulrich TA, Halsey W, Alchenberger D, Perkins TT. 2007. *Appl. Opt.* 46:421–27
57. Shaevitz JW, Abbondanzieri EA, Landick R, Block SM. 2003. *Nature* 426:684–87
58. Abbondanzieri EA, Greenleaf WJ, Shaevitz JW, Landick R, Block SM. 2005. *Nature* 438:460–65
59. Wallin AE, Salmi A, Tuma R. 2007. *Biophys. J.* 93:795–805
60. Kerssemakers JWJ, Munteanu EL, Laan L, Noetzel TL, Janson ME, Dogterom M. 2006. *Nature* 442:709–12
61. Milescu LS, Yildiz A, Selvin PR, Sachs F. 2006. *Biophys. J.* 91:1156–68
62. Milescu LS, Yildiz A, Selvin PR, Sachs F. 2006. *Biophys. J.* 91:3135–50
63. Carter BC, Vershinin M, Gross SP. 2008. *Biophys. J.* 94:306–19
64. Tolic-Norrelykke SF, Schaffer E, Howard J, Pavone FS, Julicher F, Flyvbjerg H. 2006. *Rev. Sci. Instrum.* 77:103101
65. Berg-Sorensen K, Oddershede L, Florin EL, Flyvbjerg H. 2003. *J. Appl. Phys.* 93:3167–76

A detailed discussion of how to build a high-resolution dual trap optical tweezers.

Detailed calculation of the thermal resolution limit for systems with one and two traps.

66. Berg-Sorensen K, Peterman EJG, Weber T, Schmidt CF, Flyvbjerg H. 2006. *Rev. Sci. Instrum.* 77:063106
67. Dame RT. 2005. *Mol. Microbiol.* 56:858–70
68. Amit R, Oppenheim AB, Stavans J. 2003. *Biophys. J.* 84:2467–73
69. Dame RT, Wuite GJL. 2003. *Biophys. J.* 85:4146–48
70. Dame RT, Noom MC, Wuite GJL. 2006. *Nature* 444:387–90
71. Guilford WH, Tournas JA, Dascalu D, Watson DS. 2004. *Anal. Biochem.* 326:153–66
72. K. Visscher GJBJJK. 1993. *Cytometry* 14:105–14
73. Molloy JE. 1998. *Methods Cell Biol.* 55:205–16
74. Molloy JE, Burns JE, Sparrow JC, Tregear RT, Kendrick-Jones J, White DC. 1995. *Biophys. J.* 68:S298–305
75. Nambiar R, Gajraj A, Meiners JC. 2004. *Biophys. J.* 87:1972–80
76. Kerssemakers JWJ, Janson ME, van der Horst A, Dogterom M. 2003. *Appl. Phys. Lett.* 83:4441–43
77. Footer MJ, Kerssemakers JWJ, Theriot JA, Dogterom M. 2007. *Proc. Natl. Acad. Sci. USA* 104:2181–86
78. Grier DG. 2003. *Nature* 424:810–16
79. Grier DG, Roichman Y. 2006. *Appl. Opt.* 45:880–87
80. Berg HC. 2003. *Annu. Rev. Biochem.* 72:19–54
81. Nakamoto RK, Ketchum CJ, Al-Shawi MK. 1999. *Annu. Rev. Biophys. Biomol. Struct.* 28:205–34
82. Yoshida M, Muneyuki E, Hisabori T. 2001. *Nat. Rev. Mol. Cell Biol.* 2:669–77
83. Corbett KD, Berger JM. 2004. *Annu. Rev. Biophys. Biomol. Struct.* 33:95–118
84. Charvin G, Strick TR, Bensimon D, Croquette V. 2005. *Annu. Rev. Biophys. Biomol. Struct.* 34:201–19
85. Nollmann M, Crisona NJ, Arimondo PB. 2007. *Biochimie* 89:490–99
86. Massey TH, Mercogliano CP, Yates J, Sherratt DJ, Lowe J. 2006. *Mol. Cell* 23:457–69
87. Simpson AA, Tao YZ, Leiman PG, Badasso MO, He YN, et al. 2000. *Nature* 408:745–50
88. Bryant Z, Stone MD, Gore J, Smith SB, Cozzarelli NR, Bustamante C. 2003. *Nature* 424:338–41
89. Stone MD, Bryant Z, Crisona NJ, Smith SB, Vologodskii A, et al. 2003. *Proc. Natl. Acad. Sci. USA* 100:8654–59
90. Sacconi L, Romano G, Ballerini R, Capitanio M, De Pas M, et al. 2001. *Opt. Lett.* 26:1359–61
91. Romano G, Sacconi L, Capitanio M, Pavone FS. 2003. *Opt. Commun.* 215:323–31
92. Claudet C, Bednar J. 2005. *Appl. Opt.* 44:3454–57
93. Crut A, Koster DA, Seidel R, Wiggins CH, Dekker NH. 2007. *Proc. Natl. Acad. Sci. USA* 104:11957–62
94. He H, Friese MEJ, Heckenberg NR, Rubinsztein-Dunlop H. 1995. *Phys. Rev. Lett.* 75:826–29
95. Friese MEJ, Enger J, Rubinsztein-Dunlop H, Heckenberg NR. 1996. *Phys. Rev. A* 54:1593–96
96. Friese MEJ, Nieminen TA, Heckenberg NR, Rubinsztein-Dunlop H. 1998. *Opt. Lett.* 23:1–3
97. Friese MEJ, Nieminen TA, Heckenberg NR, Rubinsztein-Dunlop H. 1998. *Nature* 394:348–50
98. Singer W, Nieminen TA, Gibson UJ, Heckenberg NR, Rubinsztein-Dunlop H. 2006. *Phys. Rev. E* 73:021911

99. Galajda P, Ormos P. 2001. *Appl. Phys. Lett.* 78:249–51
100. Bishop AI, Nieminen TA, Heckenberg NR, Rubinsztein-Dunlop H. 2003. *Phys. Rev. A* 68:033802
101. Oroszi L, Galajda P, Kirei H, Bottka S, Ormos P. 2006. *Phys. Rev. Lett.* 97:058301
102. La Porta A, Wang MD. 2004. *Phys. Rev. Lett.* 92:190801
103. Nieminen TA, Heckenberg NR, Rubinsztein-Dunlop H. 2001. *J. Mod. Opt.* 48:405–13
104. Parkin S, Knoner G, Singer W, Nieminen TA, Heckenberg NR, et al. 2007. In *Methods in Cell Biology*, ed. MW Berns, KO Greulich, pp. 525–61. New York: Academic
105. Deufel C, Forth S, Simmons CR, Dejgosha S, Wang MD. 2007. *Nat. Methods* 4:223–25
106. Gore J, Bryant Z, Nollmann M, Le MU, Cozzarelli NR, Bustamante C. 2006. *Nature* 442:836–39
107. Lionnet T, Joubaud S, Lavery R, Bensimon D, Croquette V. 2006. *Phys. Rev. Lett.* 96:178102
108. Pilizota T, Bilyard T, Bai F, Futai M, Hosokawa H, Berry RM. 2007. *Biophys. J.* 93:264–75
109. Bingelyte V, Leach J, Courtial J, Padgett MJ. 2003. *Appl. Phys. Lett.* 82:829–31
110. Keyser UF, van der Does J, Dekker C, Dekker NH. 2006. *Rev. Sci. Instrum.* 77:105105
111. Keyser UF, Koeleman BN, van Dorp S, Krapf D, Smeets RMM, et al. 2006. *Nat. Phys.* 2:473–77
112. Trepagnier EH, Radenovic A, Sivak D, Geissler P, Liphardt J. 2007. *Nano Lett.* 7:2824–30
113. Huisstede JHG, Subramaniam V, Bennink ML. 2007. *Microsc. Res. Tech.* 70:26–33
114. Weiss S. 1999. *Science* 283:1676–83
115. Toprak E, Selvin PR. 2007. *Annu. Rev. Biophys. Biomol. Struct.* 36:349–69
116. Smith SB, Finzi L, Bustamante C. 1992. *Science* 258:1122–26
117. Chu S. 1991. *Science* 253:861–66
118. Perkins TT, Quake SR, Smith DE, Chu S. 1994. *Science* 264:822–26
119. Perkins TT, Smith DE, Chu S. 1994. *Science* 264:819–22
120. Handa N, Bianco PR, Baskin RJ, Kowalczykowski SC. 2005. *Mol. Cell* 17:745–50
121. Spies M, Bianco PR, Dillingham MS, Handa N, Baskin RJ, Kowalczykowski SC. 2003. *Cell* 114:647–54
122. Bianco PR, Brewer LR, Corzett M, Balhorn R, Yeh Y, et al. 2001. *Nature* 409:374–78
123. Mameren J, Modesti M, Kanaar R, Wyman C, Wuite GJ, Peterman EJ. 2006. *Biophys. J.* 91:L78–80
124. Ishijima A, Kojima H, Funatsu T, Tokunaga M, Higuchi H, et al. 1998. *Cell* 92:161–71
125. Wallace MI, Molloy JE, Trentham DR. 2003. *J. Biol.* 2:4
126. Van Dijk MA, Kapitein LC, Van Mameren J, Schmidt CF, Peterman EJG. 2004. *J. Phys. Chem. B.* 108:6479–84
126a. Hohng S, Zhou R, Nahas MK, Yu J, Schulten K, et al. 2007. *Science* 318:279–83
127. Lang MJ, Fordyce PM, Engh AM, Neuman KC, Block SM. 2004. *Nat. Methods* 1:133–39
128. Lang MJ, Fordyce PM, Block SM. 2003. *J. Biol.* 2:6
129. Brau RR, Tarsa PB, Ferrer JM, Lee P, Lang MJ. 2006. *Biophys. J.* 91:1069–77
130. Tarsa PB, Brau RR, Barch M, Ferrer JM, Freyzon Y, et al. 2007. *Angew. Chem. Int. Ed. Engl.* 46:1999–2001
131. Banghart M, Borges K, Isacoff E, Trauner D, Kramer RH. 2004. *Nat. Neurosci.* 7:1381–86
132. Volgraf M, Gorostiza P, Numano R, Kramer RH, Isacoff EY, Trauner D. 2006. *Nat. Chem. Biol.* 2:47–52
133. Chemla YR, Aathavan K, Michaelis J, Grimes S, Jardine PJ, et al. 2005. *Cell* 122:683–92

Annual Review of Biochemistry

Volume 77, 2008

Contents

Indexes

Errata

An online log of corrections to *Annual Review of Biochemistry* articles may be found at http://biochem.annualreviews.org/errata.shtml